4-14-2021

A Pilot Study of Near-Field Airborne Particle Concentrations in Young Children Undergoing High Flow Nasal Cannula Therapy.

Elliott T. Gall
Portland State University, gall@pdx.edu

Aurélie Laguerre
Portland State University

Michelle Noelck
Oregon Health & Science University

Annalise Van Meurs
Oregon Health & Science University

Jared A. Austin
Oregon Health & Science University

Citation Details

Gall, Elliott T.; Laguerre, Aurélie; Noelck, Michelle; Van Meurs, Annalise; Austin, Jared A.; and Foster, Byron A., "A Pilot Study of Near-Field Airborne Particle Concentrations in Young Children Undergoing High Flow Nasal Cannula Therapy." (2021). *Biology Faculty Publications and Presentations*. 349.
https://pdxscholar.library.pdx.edu/bio_fac/349

Journal Pre-proof

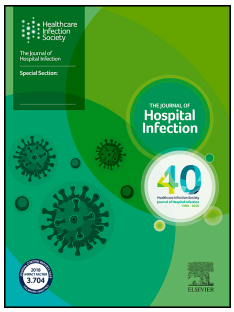

A pilot study of near-field airborne particle concentrations in young children undergoing high flow nasal cannula therapy

Elliott T. Gall, Ph.D., Aurélie Laguerre, M.S., Michelle Noelck, MD, Annalise Van Meurs, MD, Jared A. Austin, MD, Byron A. Foster, MD, MPH

PII: S0195-6701(21)00152-3

DOI: https://doi.org/10.1016/j.jhin.2021.04.002

Reference: YJHIN 6364

To appear in: *Journal of Hospital Infection*

Received Date: 19 February 2021

Revised Date: 6 April 2021

Accepted Date: 7 April 2021

Please cite this article as: Gall ET, Laguerre A, Noelck M, Van Meurs A, Austin JA, Foster BA, A pilot study of near-field airborne particle concentrations in young children undergoing high flow nasal cannula therapy, *Journal of Hospital Infection*, https://doi.org/10.1016/j.jhin.2021.04.002.

A pilot study of near-field airborne particle concentrations in young children undergoing high flow nasal cannula therapy

Elliott T. Gall, Ph.D.[a], Aurélie Laguerre, M.S.[a], Michelle Noelck, MD[b], Annalise Van Meurs, MD[b], Jared A Austin, MD,[b] Byron A. Foster, MD, MPH[b,c]

Affiliations: [a]Department of Mechanical and Materials Engineering, Portland State University, [b]Department of Pediatrics, School of Medicine, Oregon Health & Science University, [c]OHSU-PSU School of Public Health

Address correspondence to: Byron A. Foster, MD, MPH, 3181 SW Sam Jackson Park Rd, MC CDRC-P, Portland, OR 97239

Running title: Airborne particle concentrations in high flow nasal cannula therapy

Keywords: aerosols, COVID-19, respiratory illness

Funding source: The Doernbecher Philanthropy Board provided funding for the study. The funder did not participate in the work.

Financial disclosure: The authors have indicated they have no financial relationships relevant to this article to disclose.

Conflict of interest statement: The authors have indicated they have no potential conflicts of interest to disclose.

Data sharing statement: Deidentified individual participant data will not be made available. Measurements of constituents in air made in participant rooms will be made available upon reasonable request.

Contributor statements:
Dr. Gall contributed to the study conception, design, data analysis and drafting the manuscript.
Ms. Laguerre contributed to the study design, was the primary data collector, contributed to the analysis and writing the manuscript.
Dr. Noelck contributed to the study design, execution of the study and revised the manuscript.
Dr. Van Meurs contributed to the recruitment, data collection and revised the manuscript.
Dr. Austin contributed to the study design and revised the manuscript.
Dr. Foster contributed to the study conception, design, recruitment, data collection and drafting the manuscript.

Summary

Background: High flow nasal cannula therapy (HFNC) may increase aerosol generation, putting healthcare workers at risk, including from SARS-CoV-2.

Aim: This study examined whether use of HFNC increases near-field aerosols and if there is a relationship with flow rate.

Methods: Subjects aged four weeks to 24 months were recruited. Each child received HFNC therapy at different flow rates. Three stations with particle counters were deployed to measure particle concentrations and dispersion in the room: station one within 0.5 m, station two at 2 m, and station three on the other side of the room. We measured carbon dioxide (CO_2) and relative humidity. Far-field measurements were used to adjust the near-field measurements.

Findings: We enrolled ten children ranging from 6-23 months (median 9 months). Elevated CO_2 indicated the near-field measurements were in the breathing plane. Near-field breathing plane concentrations of aerosols with diameter 0.3 – 10 μm are elevated by the presence of the patient with no HFNC flow, relative to the room far-field, by 0.45 #/cm^3. While we observed variability between subjects in their emission and dispersion of particles, we did not find an association between HFNC use, at any flowrate, and near-field particle counts.

Conclusion: This method of particle sampling is feasible in hospital settings; correcting the near-patient aerosol and CO_2 levels for the room far-field may provide proxies of exposure risk to pathogens generated. In this pilot, near-patient levels of particles with a diameter between 0.3-10 μm and CO_2 were not affected by the use of HFNC.

Introduction

High flow nasal cannula therapy (HFNC) provides respiratory support for children across a range diagnoses including asthma, pneumonia and bronchiolitis. World Health Organization (WHO) guidance suggests that HFNC does not cause wide-spread dispersion of droplets from patients.[1] However, empirical data in clinical settings is lacking on whether HFNC contributes to aerosol dispersion. While children typically have more mild and even asymptomatic infections with SARS-CoV-2, respiratory disease and co-infection with other viruses have been reported.[2] HFNC has been treated as an aerosol generating procedure (AGP) in the United States given concern around particle generation, typically characterized in the health care field as droplet (≥5μm) and droplet nuclei (<5 μm).[3] Due to the increased concern for SARS-CoV-2 transmission with use of AGPs, many hospitals require the use of N-95 masks, gowns, and other personal protective equipment when patients are receiving HFNC. Determining the risk of aerosol generation from HFNC has important implications for resource management and infection control measures.

SARS-CoV-2 transmission may occur due to aerosols and large droplets, with some evidence of more widespread dispersion than typical with large droplets.[4] Most studies to date have investigated transport of large droplets from patients undergoing HFNC. Kotoda et al.[5] used a mannequin model to examine the effect of high flow nasal cannula at 60 L/min and observed large droplets (>50 μm) transported 30 cm, but not 5 m from the mannequin's face. A report examining adults coughing with and without the application of high flow nasal cannula (60 L/min) showed no significant difference in the distance of "visible" food-dye containing droplets;[6] the length scale of droplet size is not noted, though visible particles are often classified

as those >100 μm. These studies indicate large droplets are not effectively transported over long distances due to the forced air exiting the patient's nasal and oral cavity.

Studies have also employed smoke as a tracer to evaluate impacts of HFNC on room air flows and as proxies of exhaled air exposure. Hui et al.[7] used intrapulmonary smoke in a mannequin model to evaluate dispersion of exhaled air, as measured by the extent of light-scattering as a function of distance from the patient. They showed an increase in "exhaled air dispersion" from 65 mm with HFNC flow of 10 L/min to 172 mm with HFNC flow of 60 L/min. Using smoke particles as tracers and an adult human head with a lung model attached, Elshof et al.[8] examined the dispersion of 100 μm droplets using HFNC with a lung simulator. They described an estimated dispersion range of 100 μm droplets of between 18.8 and 33.4 cm from the individual using flow rates between 30-60 L/min. They also noted that HFNC increased the distance of exhaled smoke to nearly one metre under several conditions whereas a non-rebreather or Venturi mask did not influence the distance beyond normal breathing.[8]

This pilot study sought to examine whether HFNC therapy use in children generates elevated particle levels in the near-field of the patient's breathing plane. We measured concentrations of particles and carbon dioxide in hospital rooms with varying HFNC flow rates. Our study addresses several knowledge gaps concerning HFNC and particle generation and dispersion as it: i) addresses an unstudied population, children, ii) was conducted in a clinical care facility with human subjects, and iii) directly measured aerosols with diameter 0.3 - 10 μm and carbon dioxide in the near-field breathing plane and room far-field. The goals were to examine the feasibility and precision of the sampling procedure to characterize AGP in field settings, to generate data to inform the safe use of this therapy, and to inform resource management and infection control measures.

Methods

Subject eligibility and recruitment:

Subjects were recruited through fliers and email announcements. Inclusion criteria were children at a gestation-corrected age 4 weeks to 24 months and otherwise healthy. Subjects already hospitalized receiving HFNC for a respiratory illness had to have a negative SARS-CoV-2 test. We screened potential subjects for the exclusion criteria of SARS-CoV-2 exposure or symptoms, prematurity (<37 weeks) and chronic cardiac or pulmonary conditions. This study was approved as human research through the institutional IRB, and all parents provided written consent.

Experimental procedure:

Hospital rooms were chosen from available paediatric acute care rooms (patient room, hereafter, and shown in Figure 1 at a tertiary care hospital. Patient and procedure rooms had floor area ~24 m^2 and ~17 m^2, respectively and volumes of 77 m^3 and 55 m^3, respectively. CO_2 tracer decay tests conducted in patient and procedure rooms resulted in an air change rate of 8.4 and 11.0 h^{-1}, respectively (Figure S1 of Supporting Information), in general agreement with ASHRAE design recommendations for total air changes through the space. Tracer decay test analysis shown in Figure S1 uses the room steady-state CO_2 concentration prior to the injection of CO_2 as the CO_2 level entering the space from the supply air. The fraction of outdoor vs. recirculated air is unknown, though we note guidelines are 2 and 3 outdoor air changes per hour, respectively, for patient and procedure rooms.[9] Air entering the rooms is treated with MERV10 and MERV15 filtration. Figure 1 shows the configuration of the supply and return register in the patient rooms, where most experiments took place. In patient rooms, the supply and return registers are approximately 1.2 m apart. In the procedure room, the registers are approximately

2.5 m apart. For the two patients with respiratory illness who were part of the study measurements were made in a negative pressure room, with an additional negative flow duct on the wall abutting the floor, approximately 3 m from the patient. We did not observe cycling of the HVAC system in patient or procedure rooms during measurements.

Subjects were placed on a hospital bed with a parent in the room, with the parent wearing a cloth or surgical mask at all times. A high-flow nasal cannula system (Fisher and Paykel's Optiflow Junior, circuit RT 330) with an appropriately sized nasal cannula for each subject's size and weight was set-up by a qualified respiratory therapist.

Ambient air in the hospital room was first sampled with the door closed and no patient present (background condition) for 15 minutes. The child was then connected to the HFNC, flow was then increased from 0 to 0.5 L/kg/min, to 1 L/kg/min then finally to 2 L/kg/min, then back to 0 L/kg/min and repeated the cycle one more time for a total of two measurements per subject at each flow rate. Each cycle lasted about seven minutes. An experimental timeline is shown in Figure 1. HFNC air was heated to approximately 37°C and humidified. No supplementary oxygen was provided. We conducted a positive control following the completion of the protocol twice over the course of the study. In this control, particle and CO_2 levels were measured in the breathing plane ~0.5 m from the nasal/oral cavity of member of the research team during and after volitional coughing.

We recruited ten children ranging from 6-23 months (median nine months) and their parents to participate in the study between September and November 2020. The median weight of participants was 9.8 kg (range 7.3-14.0 kg). The flow rates were calculated for each child at 0.5 L/kg/min, 1 L/kg/min and 2 L/kg/min with a max flow rate in this study of 25 L/min, which two of the participants reached. See Table S1 for flowrates for each patient as well as

environmental conditions during measurements. Two patients (P02 and P03) are excluded from subsequent analysis as measurements occurred during periods of extremely elevated outdoor air pollution due to wildfires in the region. For patients with respiratory illness (P08 and P10), we were not able to vary the HFNC flowrate and have no background measurements.

Particle and carbon dioxide measurement:

Three sampling stations were deployed in the room of each study participant prior to their arrival, excepting P08 and P10 who were present prior to sampling. The main sampling location (station 1, Figure 1) was set within the patient's breathing plane at a distance of ~0.5 m. This main sampling station was set up similar to O'Neil et. al[10]. An optical particle sizer (TSI/OPS 3330) and scanning mobility particle sizer (TSI/NanoScan SMPS 3910) counted particles ranging from 0.01 to 10 μm at a time resolution of one-minute. A condensation particle counter (TSI, P-Trak 8525) measured particles ranging 0.02 to 1 μm in one second time interval. Isokinetic sampling (constant flow rate into the sampling outlet) was not possible due to the variability in airflows in the room and due to the exhalations of the patient. A CO_2 analyzer (LICOR LI-820) measured CO_2 levels in one second intervals. A temperature and relative humidity sensor (Onset, S-THB-M002) measured in one-minute interval.

Two additional sampling stations (station 2 and 3, Figure 1) were installed to monitor the room. Each station included a particle counter (Purple Air, PA-II-SD), measuring particle number concentration in six size bins from 0.3 - 10 μm and recording every 80 seconds, and a CO_2 sensor (Onset, MX1102) recording every minute. In this study, we normalize the data reported by station 1 (near-field) to that of station 3 (far-field), which we take as the ambient, mixed room particle and CO_2 level. Note that we lacked particle number concentrations <0.3 μm in the station 2 and 3 locations; for this reason and the focus of the work on vectors > 0.1 μm in

diameter, this investigation subsequently focuses on particulate matter with aerodynamic diameter 0.3 – 10 μm ($PM_{0.3\text{-}10}$), the range most likely to explain small particle transmission of SARS-CoV-2 .

Field co-location of instruments:

The particle counters and CO_2 sensors in stations 1 and 3 were co-located during the background period, when the room was unoccupied for 15 min. We used these periods to develop correction factors that were applied to the far-field (station 3) sensor during periods of participant occupancy. The OPS size bins were averaged to match the six bins of the PA. A correction factor for each size bin was calculated as in equation 1:

$$CF(x) = \frac{\overline{PM_{OPS}(x)}}{\overline{PM_{PA}(x)}} \quad \text{eq. 1}$$

where $CF(x)$ is the correction factor for size bin x, $\overline{PM_{OPS}(x)}$ is the time-averaged OPS value in size bin x, and $\overline{PM_{PA}(x)}$ is the time-averaged PA value in size bin x. We used a linear regression to correct the values given by the far-field CO_2 sensor (Onset MX1102) to that of the LICOR LI-820 during the 15-minute background period.

Calculations of ΔPM and ΔCO2:

To account for the changing concentration of $PM_{0.3\text{-}10}$ and CO_2 in the room due to processes other than the patient undergoing HFNC, we normalize the near-field (station 1) measurements to that of the far-field (station 3). We report the normalized metrics as $\Delta PM_{0.3\text{-}10}$ (#/cm^3) and ΔCO_2 (ppm) calculated as shown in equations 2 and 3:

$$\Delta PM(t) = PM_{near}(t) - PM_{far}(t) \quad \text{eq. 2}$$

$$\Delta CO_2(t) = CO_{2\,near}(t) - CO_{2\,far}(t) \quad \text{eq. 3}$$

where $PM_{near}(t)$is the time-varying particle concentration at station 1 (#/cm^3), $PM_{far}(t)$is the corrected (i.e., eq. 1) particle concentration at station 3, $CO_{2\,near}(t)$is CO_2 concentration at station 1 (ppm), and $CO_{2\,far}(t)$is the corrected CO_2 concentration at station 3 (ppm).

Statistical testing:

We evaluate statistical significance of differences in means of $\Delta PM_{0.3\text{-}10}$ and in medians of ΔCO_2 across HFNC flow rates using a student t-test for $\Delta PM_{0.3\text{-}10}$ and a Wilcoxon rank sum test for ΔCO_2. Tests for normality and statistical testing employed the average of each HFNC condition conducted in duplicate across the six healthy subjects (i.e., 12 independent samples of $\Delta PM_{0.3\text{-}10}$ and ΔCO_2 for each condition).

Results:

Measurements of particle concentrations, CO_2, temperature and relative humidity (RH) for two example patients are shown in Figure 2. In the top panel, room particle concentrations are reported in the near-field breathing plane (station 1) and far-field (station 3) of the room, with the second panel showing the difference ($\Delta PM_{0.3\text{-}10}$). For patient 01, near-field is generally higher than far-field, resulting in positive $\Delta PM_{0.3\text{-}10}$. We also observed sharp spikes in ΔCO_2. This implies measurements captured patient exhalations, as the source of CO_2 in the room is the patient. Conversely, in Patient 06 there are lower levels of particles in the near-field vs. far-field, resulting in a generally negative $\Delta PM_{0.3\text{-}10}$. This is possibly due to a low particle generation rate for this patient, room mixing conditions, and/or other sources of particles during this experiment (e.g., changes in the room airflows due to HVAC operation or movement by the parent around the room). For positive controls we observe elevated particle and CO_2 concentrations following the volitional cough, shown at elapsed time ~100 min for both patients. A child's parent, present in the room during the study, may contribute to the CO_2 and aerosols measured in the near-field.

However, instruments were installed with inlet targeting the breathing plane of the child only. This possible confounder is present consistently across each subject's varied HFNC conditions, as the parent was present with the child for the duration of the test.

Distributions of ΔPM and ΔCO_2 are shown in Figure 3 across baseline conditions (HFNC at 0 L/kg/min), HFNC with flow, and positive control. Similar plots are shown for size-resolved particles in Figure S2 of the Supporting Information. Shown in Figure 3 are the measurements of particles and CO_2 made with 1-min time resolution. Across all six patients, we observe that the presence of the patient alone (i.e., baseline) results in an increase in the near-field PM (i.e., median $\Delta PM_{0.3\text{-}10}$ is positive). Presence of HFNC flow does not significantly change the mean $\Delta PM_{0.3\text{-}10}$ compared to the baseline condition (see *p*-values in Table S2). Measurements of ΔCO_2 made for the six patients shown in Figure 3 indicate that median ΔCO_2 is consistently positive. This implies that near-field measurements generally occurred in the exhalations of the patient. Again, no significant change is observed with HFNC flow compared to the baseline condition (see *p*-values in Table S2). The volitional cough positive control resulted in substantially higher $\Delta PM_{0.3\text{-}10}$ and ΔCO_2.

While median $\Delta PM_{0.3\text{-}10\text{ and }}\Delta CO_2$ are consistently positive, there existed across-subject variability in $\Delta PM_{0.3\text{-}10\text{ and }}\Delta CO_2$. For example, Patients 01, 05, 07, and 09 had consistently positive $\Delta PM_{0.3\text{-}10}$ while Patients 04 and 06 were consistently negative (Figure 4a). Values of ΔCO_2 were more consistently positive than $\Delta PM_{0.3\text{-}10}$, as shown in Figure 4b, though again, there exists variability across subjects.

In Figure 5, we show the results of $\Delta PM_{0.3\text{-}10\text{ and }}\Delta CO_2$ for the two patients recruited who had respiratory illness; results are limited to only one flowrate as we did not alter the patients' care directives. Since background measurements were infeasible, correction factors were used

from healthy patient studies conducted on the same respective days. As in healthy patients, we observe variability in median $\Delta PM_{0.3\text{-}10}$, with P08 negative and P10 positive. In contrast, ΔCO_2 for both patients is greater than zero, implying measurements occurred in patient breathing planes.

Discussion:

Results of this pilot study indicate, across patients, that HFNC does not appear to be substantial source of aerosol generation or dispersion in the near-field beyond that of the patient's presence. Human breath contains particles - while results are variable across time for each patient and between patients, the median $\Delta PM_{0.3\text{-}10}$ reported in this measurement is roughly consistent with the previous measurements of particle number concentrations in human breath. Johnson et al.[11] report particle levels in speaking and coughing emissions in the size range of 0.5 - 1000 μm of 0.16 #/cm^3 and 0.22 #/cm^3, respectively. In our study, the complex fluid mechanics occurring in the patient's breathing plane due to exhaled breath, HFNC airflow, and the room airflows complicate further theoretical calculations of particle concentrations or emission rate originating from the patient. Humans also generate particles from activity.[12] Particles originating from the respiratory system versus patient movement, for example, cannot be differentiated here.

Median values of $\Delta PM_{0.3\text{-}10}$ decreased slightly, though not statistically significantly, with increasing HFNC flow rate. We speculate this may be the result of enhanced mixing between forced air from subject and room air with higher velocities at higher HFNC flow conditions. There are no statistically significant differences across $\Delta PM_{0.3\text{-}10}$ or ΔCO_2 for any comparison of flow conditions. We set the threshold of significance as $p < 0.0083$ for 95% confidence with Bonferonni correction for multiple comparisons. Calculated *p*-values are shown in the Table S2 of the Supporting Information.

Results shown in Figure 4 reveal high variability in near-patient concentrations of PM and CO_2. The explanation for the mechanism behind these observations is beyond the scope of this paper, though we speculate it is possible that patients with negative $\Delta PM_{0.3\text{-}10}$ may be low emitters of particles or positioned in the space such that enhanced particle deposition is occurring in the turbulence generated from airflows interacting with the patient and associated equipment (bedding, instruments, etc.). Particles also deposit in the respiratory system.[13] Patient 06 and Patient 04 measurements were conducted during relatively high room background PM levels, perhaps contributing to the negative $\Delta PM_{0.3\text{-}10}$ observed. We note that prior studies have observed large variability in particle emission rate and concentrations in exhalations of humans during breathing and speaking.[14–18] There is debate on the size of particles that are considered infectious, with droplet nuclei playing a larger role than previously considered[19] – one strength of our study is that we were able to measure a broad range of potentially infectious particles, including droplet nuclei.

Differences in near-field to far-field CO_2 were larger and more pronounced than for PM. CO_2 levels in human breath are ~100x higher than ambient levels (~38,000 vs. 400 ppm).[20] In contrast, particle concentrations in human breath in the size range 0.3 - 10 μm are expected to be similar or lower than background levels measured in patient rooms.[14] There also exists large variation in particle generation rates during breathing and coughing, with the presence of a respiratory infection causing increased particle generation rate.[21]

In contrast to the variability in $\Delta PM_{0.3\text{-}10}$ shown, ΔCO_2 is variable but more consistently positive (Figure 4b), implying that measurements were generally made in the breathing planes of the patients. There does not appear to be a relationship between elevated ΔCO_2 and $\Delta PM_{0.3\text{-}10}$, that is, high values of ΔCO_2 do not necessarily associate with high $\Delta PM_{0.3\text{-}10}$. For example, P01

had the highest ΔCO_2 for three of four HFNC flow conditions, but $\Delta PM_{0.3\text{-}10}$ was consistently near the median value reported. Again, we speculate that this is a result of differences in particle generation across subjects that are not related to metabolism (e.g., unknown physiological factors that have been previously suggested as explaining "superemission" of aerosol during speech[15]).

Our limited sample of two patients with respiratory illness shown in Figure 5 demonstrates variability in near-field elevations of particles, with Patient 10 showing greater $\Delta PM_{0.3\text{-}10}$ than all healthy patients by a substantial margin. This appears largely driven by a difference in the behavior of particles 0.3 – 0.5 μm, as this size range dominated the particle number concentration. For both patients with respiratory infection we note there was an elevation in $\Delta PM_{0.5\text{-}1}$, a size range that a prior study shows is significantly elevated during a respiratory infection.[22] We did not have the ability to vary HFNC flowrate for these subjects, and so lack a baseline period of no HFNC flow for comparison.

HFNC is also widely used in adult patients. We suspect adults could have greater dispersion as typical volumes used (60 L/min) are much higher, even scaled for tidal volume, though strongly suggest the experiment should be completed.

Conclusions:

In this pilot study, our measurements indicate near-field (~0.5 m) breathing plane concentrations of aerosol and carbon dioxide are elevated by the presence of the patient with no HFNC flow. Addition of HFNC flow in the range of 0.5 - 2 L/kg/min did not significantly change the magnitude of near-field PM or CO_2, corrected for the room far-field. These findings indicate that HFNC use in children may not substantially elevate clinician aerosol exposures greater than the presence of the patient alone, though we observe variability across patients that warrants consideration and further study. Our pilot study consisted of a small sample size and

thus proof of clinical insignificance is not possible with the present dataset. Future studies can use these pilot data to inform experimental design to ensure sufficient power in comparing measurements of CO_2 and aerosols in a field setting that are subject to substantial variability. For example, a sample size of ~165 patients would be necessary to achieve power = 0.9 in comparing average $\Delta PM_{0.3\text{-}10}$ across baseline and 0.5 L/kg/min HFNC conditions. In addition to larger scale studies, future studies should evaluate potential aerosol generating procedures in controlled settings where particle emission rates can be calculated; these data would enable dispersion modeling of particles emitted by patients. It is also worth noting that measurements of aerosols and CO_2 serve as proxies for exposure to a pathogen of concern. Relating measurements of CO_2 and aerosols to likelihood of disease transmission is out of the scope of this pilot study. Such efforts should consider the known large variability in emission rates of viruses across humans for activities like breathing and speech.[23] Further study of the impacts of HFNC on particle generation and dispersion in patients with respiratory illness is warranted.

References:

1. WHO. *Clinical Management of Severe Acute Respiratory Infection When Novel Coronavirus (2019-NCoV) Infection Is Suspected*. World Healthy Organization; 2020. Accessed December 5, 2020. https://www.who.int/publications-detail-redirect/clinical-management-of-covid-19

2. Wu Q, Xing Y, Shi L, Li W, Gao Y, Pan S et al. Coinfection and Other Clinical Characteristics of COVID-19 in Children. *Pediatrics*. 2020;146(1). doi:10.1542/peds.2020-0961

3. Agarwal A, Basmaji J, Muttalib F, Granton D, Chaudhuri D, Chetan D et al. High-flow nasal cannula for acute hypoxemic respiratory failure in patients with COVID-19: systematic reviews of effectiveness and its risks of aerosolization, dispersion, and infection transmission. *Can J Anaesth*. Published online June 15, 2020:1-32. doi:10.1007/s12630-020-01740-2

4. Azimi P, Keshavarz Z, Laurent JGC, Stephens B, Allen JG. Mechanistic transmission modeling of COVID-19 on the Diamond Princess cruise ship demonstrates the importance of aerosol transmission. *PNAS*. 2021;118(8). doi:10.1073/pnas.2015482118

5. Kotoda M, Hishiyama S, Mitsui K, Tanikawa T, Morikawa S, Takamino A et al. Assessment of the potential for pathogen dispersal during high-flow nasal therapy. *J Hosp Infect*. 2020;104(4):534-537. doi:10.1016/j.jhin.2019.11.010

6. Loh N-HW, Tan Y, Taculod J, Gorospe B, Teope AS, Somani J et al. The impact of high-flow nasal cannula (HFNC) on coughing distance: implications on its use during the novel coronavirus disease outbreak. *Can J Anaesth*. 2020;67(7):893-894. doi:10.1007/s12630-020-01634-3

7. Hui DS, Chow BK, Lo T, Tsang OTY, Ko FW, Ng SS et al. Exhaled air dispersion during high-flow nasal cannula therapy versus CPAP via different masks. *Eur Respir J*. 2019;53(4). doi:10.1183/13993003.02339-2018

8. Elshof J, Hebbink RHJ, Duiverman ML, Hagmeijer R. High-flow nasal cannula for COVID-19 patients: risk of bio-aerosol dispersion. *Eur Respir J*. 2020;56(4). doi:10.1183/13993003.03004-2020

9. Air | Appendix | Environmental Guidelines | Guidelines Library | Infection Control | CDC. Published July 22, 2019. Accessed March 30, 2021. https://www.cdc.gov/infectioncontrol/guidelines/environmental/appendix/air.html

10. O'Neil CA, Li J, Leavey A, Wang Y, Hink M, Wallace M et al. Characterization of Aerosols Generated During Patient Care Activities. *Clin Infect Dis*. 2017;65(8):1335-1341. doi:10.1093/cid/cix535

11. Johnson GR, Morawska L, Ristovski ZD, Hargreaves M, Mengersen K, Chao CYH et al. Modality of human expired aerosol size distributions. *Journal of Aerosol Science*. 2011;42(12):839-851. doi:10.1016/j.jaerosci.2011.07.009

12. Ferro AR, Kopperud RJ, Hildemann LM. Source strengths for indoor human activities that resuspend particulate matter. *Environ Sci Technol*. 2004;38(6):1759-1764. doi:10.1021/es0263893

13. Hinds WC. *Aerosol Technology: Properties, Behavior, and Measurement of Airborne Particles*. 2 edition. Wiley-Interscience; 1999.

14. FAIRCHILD CI, STAMPFER JF. Particle Concentration in Exhaled Breath. *American Industrial Hygiene Association Journal*. 1987;48(11):948-949. doi:10.1080/15298668791385868

15. Asadi S, Wexler AS, Cappa CD, Barreda S, Bouvier NM, Ristenpart WD. Aerosol emission and superemission during human speech increase with voice loudness. *Scientific Reports*. 2019;9(1):2348. doi:10.1038/s41598-019-38808-z

16. Edwards DA, Man JC, Brand P, Katstra J, Sommerer K, Stone H et al. Inhaling to mitigate exhaled bioaerosols. *PNAS*. 2004;101(50):17383-17388. doi:10.1073/pnas.0408159101

17. Papineni RS, Rosenthal FS. The Size Distribution of Droplets in the Exhaled Breath of Healthy Human Subjects. *Journal of Aerosol Medicine*. 1997;10(2):105-116. doi:10.1089/jam.1997.10.105

18. Fabian P, McDevitt JJ, DeHaan WH, Fung R, Cowling B, Chan KH et al. Influenza Virus in Human Exhaled Breath: An Observational Study. *PLOS ONE*. 2008;3(7):e2691. doi:10.1371/journal.pone.0002691

19. Fennelly KP. Particle sizes of infectious aerosols: implications for infection control. *The Lancet Respiratory Medicine*. 2020;8(9):914-924. doi:10.1016/S2213-2600(20)30323-4

20. Rudnick SN, Milton DK. Risk of indoor airborne infection transmission estimated from carbon dioxide concentration. *Indoor Air*. 2003;13(3):237-245.

21. Lindsley WG, Pearce TA, Hudnall JB, Davis KA, Davis SM, Fisher M et al. Quantity and Size Distribution of Cough-Generated Aerosol Particles Produced by Influenza Patients During and After Illness. *J Occup Environ Hyg*. 2012;9(7):443-449. doi:10.1080/15459624.2012.684582

22. Lee J, Yoo D, Ryu S, Ham S, Lee K, Yeo M et al. Quantity, Size Distribution, and Characteristics of Cough-generated Aerosol Produced by Patients with an Upper Respiratory Tract Infection. *Aerosol Air Qual Res*. 2019;19(4):840-853. doi:10.4209/aaqr.2018.01.0031

23. Edwards DA, Ausiello D, Langer R, Salzman J, Devlin T, Beddingfield B et al. Exhaled aerosol increases with COVID-19 infection, age, and obesity. *PNAS*. 2021;118(8). doi:10.1073/pnas.2021830118

403 **Figure captions**
404
405 **Figure 1.** Panel A) Layout of patient room and sampling locations with stars R and S
406 respectively corresponding to the return and supply registers on the ceiling, and Panel B)
407 Timeline of experiments for each patient
408
409

Figure 2. Example particle and CO_2 concentrations in the breathing plane of two patients. Shading annotations shows the condition of the experimental protocol. Note the difference in scales for PM and ΔPM across the two subjects.

Figure 3. Panel A) Distributions of measured $\Delta PM_{0.3-10}$ and Panel B) ΔCO_2 for six patients involved in this study. Centerline of box plots report median, extent of box is 25^{th} and 75^{th} percentiles, and whisker designates upper and lower extent of outliers in the distribution. Note that Δ indicates reported measurements are the difference between the near-field breathing plane and the coincident ambient room concentration (far-field), as explained in the text.

Figure 4. Panel A) Across-subjects variability in $\Delta PM_{0.3\text{-}10}$ and Panel B) ΔCO_2. Each bar is the median across 1-min averaged measurements at each HFNC flow condition for the indicated subject. The error bars show the range across the 1-min averaged measurements (max-min). The upper error bar for P01 at 0.5 L/kg/min extends to 310 ppm, not shown for figure clarity.

Figure 5. Size resolved $\Delta PM_{0.3\text{-}10}$ and ΔCO_2 for two patients with diagnosed respiratory illness. Patient 08 was 3 months old and HFNC flowrate of 3 LPM, Patient 10 was 24 months with HFNC flowrate of 15 LPM. Bars show median values of 1-min averaged measurements while error bars show the range across a 10-min monitoring period.

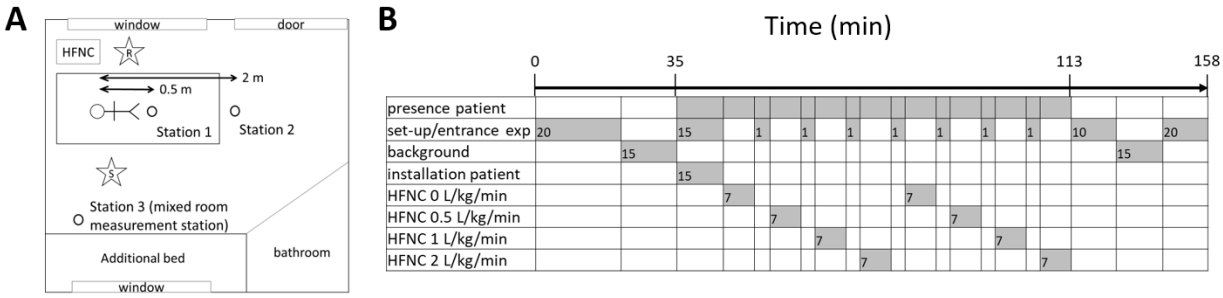

Figure 1. Panel A) Layout of patient room and sampling locations with stars R and S corresponding respectively to the return and supply registers on the ceiling, and Panel B) Timeline of experiments for each patient

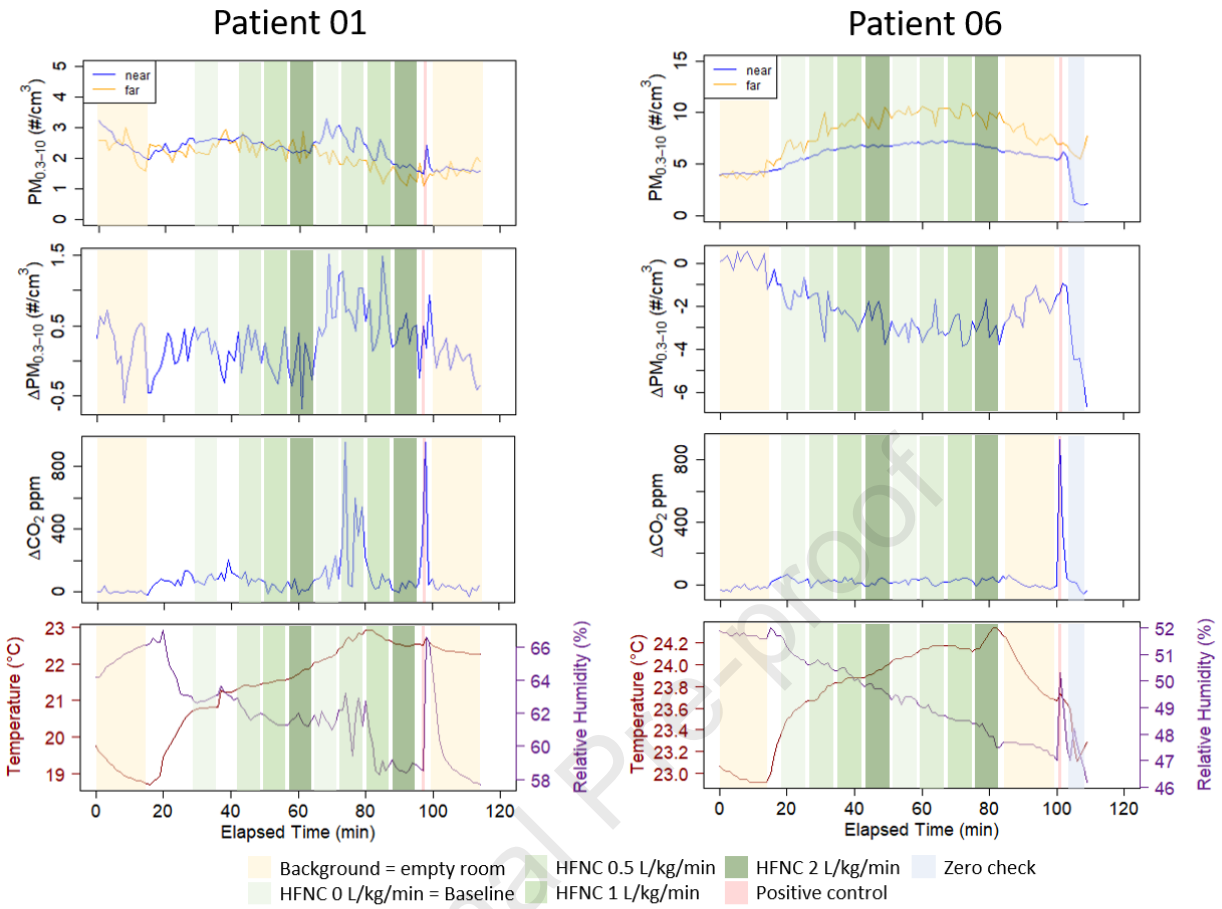

Figure 2. Example particle and CO_2 concentrations in the breathing plane of two patients. Shading annotations shows the condition of the experimental protocol. Note the difference in scales for PM and ΔPM across the two subjects.

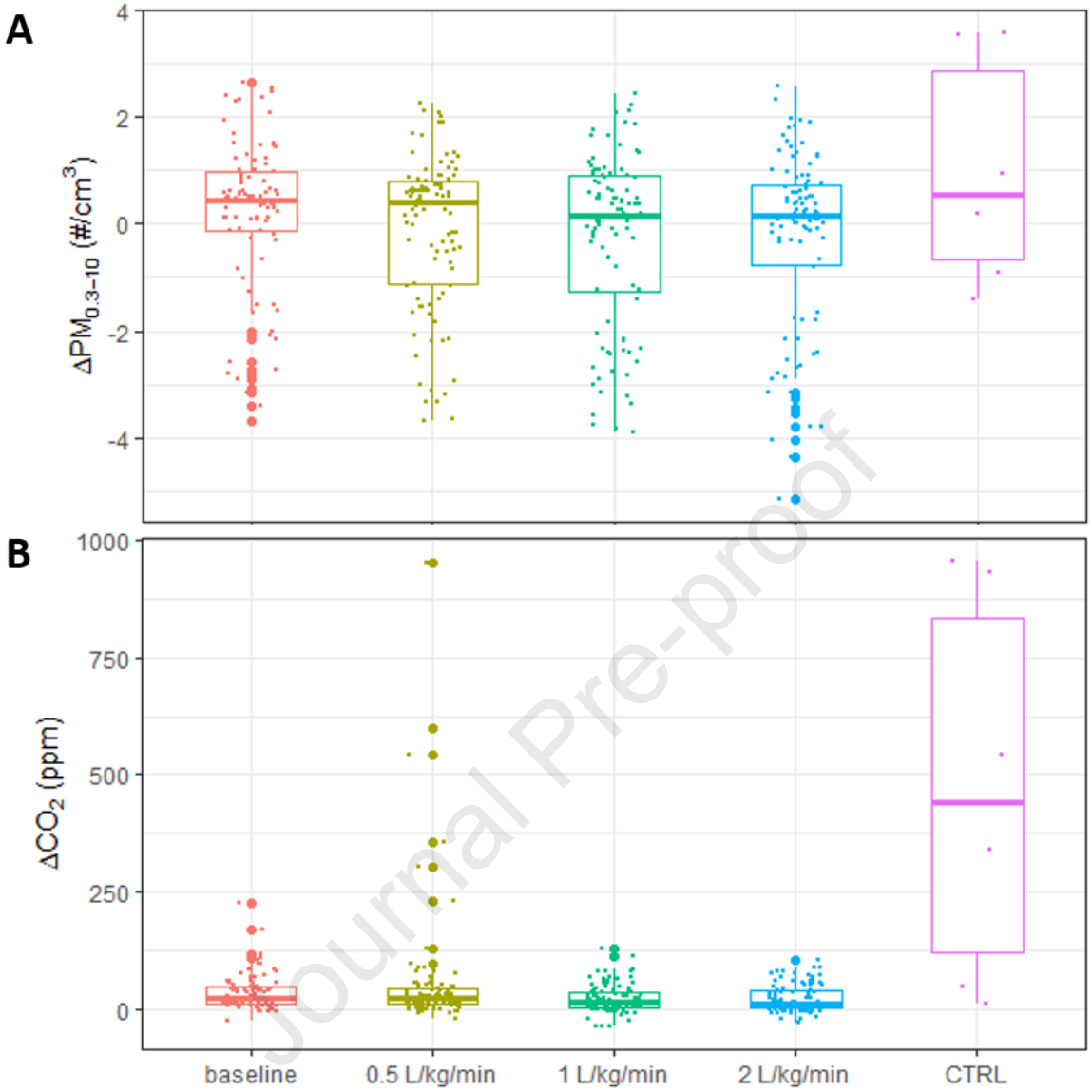

Figure 3. Panel A) Distributions of measured $\Delta PM_{0.3\text{-}10}$ and Panel B) ΔCO_2 for six patients involved in this study. Centerline of box plots report median, extent of box is 25th and 75th percentiles, and whisker designates upper and lower extent of outliers in the distribution. Note that Δ indicates reported measurements are the difference between the near-field breathing plane and the coincident ambient room concentration (far-field), as explained in the text.

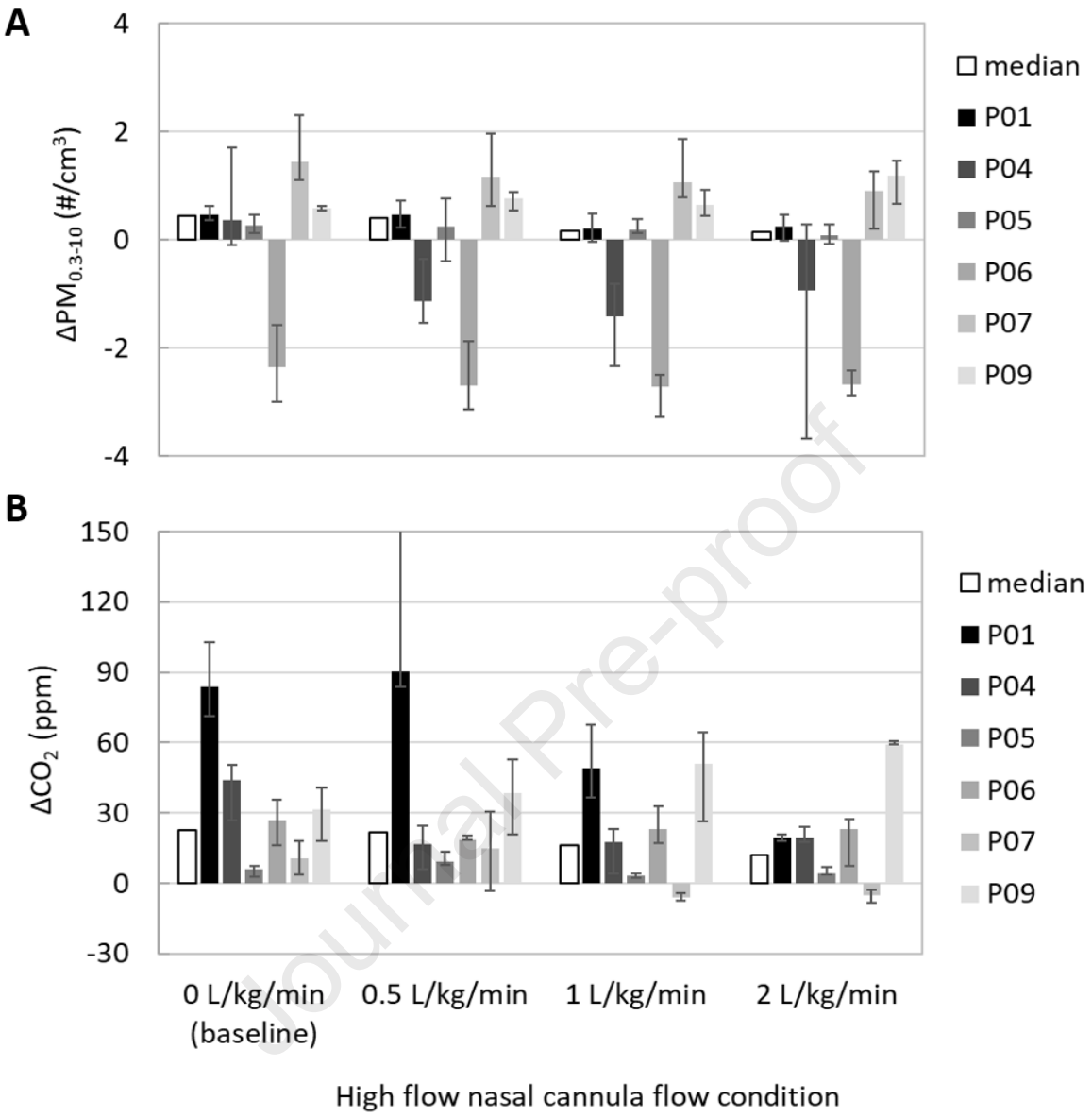

Figure 4. Panel A) Across-subjects variability in $\Delta PM_{0.3\text{-}10}$ and Panel B) ΔCO_2. Each bar is the median across 1-min averaged measurements at each HFNC flow condition for the indicated subject. The error bars show the range across the 1-min averaged measurements (max-min). The upper error bar for P01 at 0.5 L/kg/min extends to 310 ppm, not shown for figure clarity.

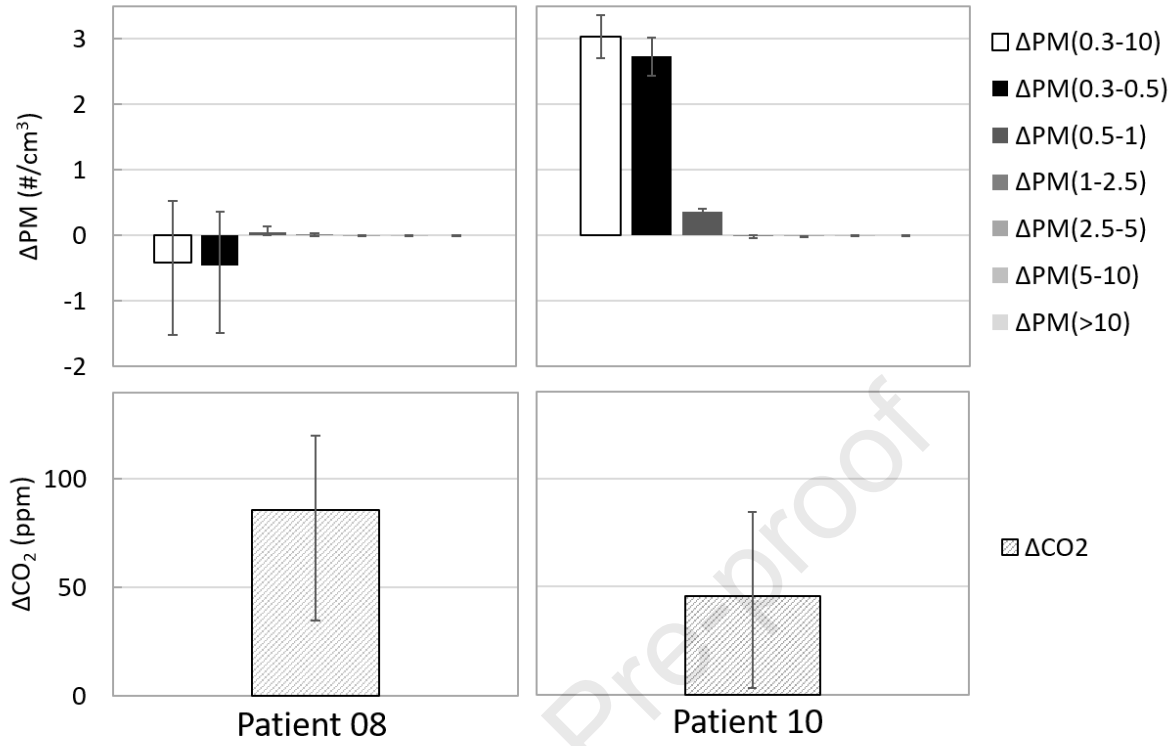

Figure 5. Size resolved $\Delta PM_{0.3\text{-}10}$ and ΔCO_2 for two patients with diagnosed respiratory illness. Patient 08 was 3 months old and HFNC flowrate of 3 LPM, Patient 10 was 24 months with HFNC flowrate of 15 LPM. Bars show median values of 1-min averaged measurements while error bars show the range across a 10-min monitoring period.